ADVANCED FUNCTIONAL MATERIALS
www.afm-journal.de

Bioinspired Water-Vapor-Responsive Organic/Inorganic Hybrid One-Dimensional Photonic Crystals with Tunable Full-Color Stop Band

By *Zhanhua Wang, Junhu Zhang, Jing Xie, Chuang Li, Yunfeng Li, Sen Liang, Zhicheng Tian, Tieqiang Wang, Hao Zhang, Haibo Li, Weiqing Xu,* and *Bai Yang**

Bioinspired organic/inorganic hybrid one-dimensional photonic crystals (1DPCs) are prepared by alternating thin films of titania and poly(2-hydroxyethyl methacrylate-co-glycidyl methacrylate) (PHEMA-co-PGMA) by spin-coating, which is a simple, reproducible, and low-cost approach. Their optical properties are tuned by changing the number of layers, incident angles, and the thickness of the layers. The color of the 1DPCs can span the entire visible spectral range when the period or the refractive index is changed. Due to the response of PHEMA-co-PGMA to water vapor, the 1DPCs possess fast water-vapor responsiveness and reversible full-color switching. The color of the 1DPCs varies from blue to green, yellow, orange, and red under differing humidities, covering the whole visible range. At high water-vapor concentrations, the color of the 1DPCs rapidly changes from blue to red and comes back to the original state immediately after exposure to air; this behaviour is like that of some animals in nature. The repeatability of the reversible response of the 1DPCs to water vapor is perfect and can be repeated more than 100 times. The as-prepared 1DPCs successfully combine structural color and water-vapor sensitivity, which is promising for use as materials for colorful detection across the full color range.

1. Introduction

Photonic crystals, which are structures that present periodic modulation of the refractive index, have been a subject of much interest in the materials science community for many years.[1,2] According to the variation of refractive index and period in space, photonic crystals can be classified as one-dimensional, two-dimensional, and three-dimensional. They display potential applications in telecommunications,[3] photocatalysts,[4] photovoltaics,[5] and displays.[6] Furthermore, by combining them with stimuli-responsive materials that respond to external stimuli, such as pH, ionic strength, solvent, vapor, temperature, light, and so on, photonic crystals have been developed for chemical and biological sensing; this range of applications utilizes their variety of microstructures and optical properties and their interactions with the environment.[7]

A variety of animals in nature present iridescent color by the presence of photonic crystal structures on the surface of their bodies; so-called structural color.[8] Structural color from photonic crystals includes crystal multilayer interference, diffraction grating, and three-dimensional photonic crystals.[9] Additionally, structural color is not always static; some kinds of structural color can change with external stimuli. For example, the color of a damselfish can change between green and blue;[10] the reflective stripes on a paradise whiptail's head and body can change from blue to red in 0.25 s and recover to blue in 5 s when the environmental osmotic pressure changes.[11] Structural color changes on the surfaces of animals are caused by the introduction of physical or chemical stimuli which change the refractive index and/or period of the materials. By benefiting from these lessons, tunable structural color has been achieved by preparing many kinds of responsive photonic crystals,[12] which have potential applications in optical/memory devices and chemical/biochemical sensors.[7,13]

Up to now, only 3D and 2D photonic crystals have been studied extensively due to the development of state-of-the-art lithographic techniques and the perfection of self-assembly methods for the generation of high-quality opal and inverse-opal structures.[14] However, one-dimensional photonic crystals (1DPCs) have received less attention because of a lack of dynamic viability and the decades-old dependence on complex top-down techniques for fabrication of 1DPCs, although structural color from 1DPCs does exist extensively in nature.[11,15] In recent years, due to the development of simple bottom-up techniques, a lot of functional 1DPCs have been prepared using bottom-up approaches based on dip- or spin-coating.[16] 1DPCs demonstrate special kinds of crystal multilayer interference, which is caused by alternating layers of high and low-refractive-index materials with planar interfaces between each

[*] Z. Wang, Dr. J. Zhang, J. Xie, C. Li, Y. Li, S. Liang, Z. Tian, T. Wang, H. Zhang, H. Li, W. Xu, Prof. B. Yang
State Key Laboratory of Supramolecular Structure and Materials
College of Chemistry
Jilin University
Changchun 130012, P. R. China
E-mail: byangchem@jlu.edu.cn

DOI: 10.1002/adfm.201001195

© 2010 WILEY-VCH Verlag GmbH & Co. KGaA, Weinheim

pair of layers. Besides, if 1DPCs are prepared containing stimuli-responsive materials or porous materials, their optical properties can be tuned to generate bioinspired, tunable structural color by introducing changing external stimuli. Recently, many kinds of materials have been used to prepare functional 1DPCs which possess good optical properties and tunable, bioinspired structural color. These materials include inorganic materials,[17–21] organic/inorganic hybrid materials,[22] and polymer or organic materials.[23–27] The inorganic materials used include mesoporous metal oxides,[17] amorphous inorganic nanoparticles,[18] clay,[19] porous silicon,[20] and porous anodic aluminum oxide.[21] Polymer and organic materials include cholesteric liquid crystals,[23] block copolymer[24]and polymer multilayer by layer-by-layer,[25] coextrusion,[26] and holographic photopolymerization.[27] These chemically tunable 1DPCs open up applications in controllable release,[28] displays,[29] sensors,[17–21,30–32] lasers,[33] and so on.

1DPCs made up of inorganic materials are stable and their optical properties can be tuned by filling the interspace with gases or solvents. However, any changes in optical properties are small because the period is difficult to change. Due to the small refractive-index difference between different kinds of polymers, 1DPCs consisting of polymer and organic materials must have many layers to achieve an obvious stop band, which influences their optical responsive properties greatly. Furthermore, the preparation method is also complicated. Organic/inorganic hybrid 1DPCs possess good stability and excellent optical properties because of the large difference in refractive indexes. Their optical properties can be tuned largely when the organic layer is active. Gleason and co-workers reported an organic/inorganic hybrid 1DPC which has a high water-vapor sensitivity with a response time of less than 0.3 s, made by using the vapor-deposition method.[22a] Thomas and co-workers prepared an organic/inorganic hybrid one-dimensional photonic gel by self-assembly of block copolymers and using the sol–gel method.[22c] However, finding a simple way to prepare organic/inorganic hybrid 1DPCs with reversible full-color switching is highly desirable at present.

In this paper, we report a simple and low-cost method to fabricate bioinspired organic/inorganic hybrid 1DPCs by using alternating thin films of titania and poly(2-hydroxyethyl methacrylate-co-glycidyl methacrylate) (PHEMA-co-PGMA) by spin-coating. The color of the 1DPCs prepared can be changed from blue to red, through the whole visible spectral range, by simply controlling the layer thickness. Furthermore, the optical properties of the 1DPCs can also be tuned by changing the number of layers, incident angles, and refractive index. Meanwhile, due to the response of PHEMA-co-PGMA to water vapor, 1DPCs prepared in this way possess fast water-vapor responsiveness and reversible full-color switching. The colors of 1DPCs can be varied from blue to green, yellow, orange, and red by changing the concentration of water vapor, thereby covering the whole visible range. At high vapor concentration, the photonic stop band of the 1DPCs changes quickly from blue to red and comes back to the original state immediately after exposure to air, which is like the behavior of some animals. The water-vapor- responsive behavior of 1DPCs is reversible and can be repeated more than 100 times. The as-prepared 1DPCs successfully combine structural color and water-vapor sensitivity, and they are promising materials for colorful detection in the chemical and biological fields.

2. Results and Discussion

2.1. Preparation and Characterization of 1DPCs

Bioinspired organic/inorganic hybrid 1DPCs were achieved by using alternating titania and PHEMA-co-PGMA by spin-coating (see **Scheme 1**). The titania layer is chosen because of its higher refractive index when compared with the polymer layer, and the simple preparation method. Furthermore, it can also form uniform films easily. The effective refractive indexes of the polymer and titania layers were determined by spectroscopic ellipsometry to be 1.512 and 1.831, respectively. The polymer precursor was synthesized by solution radical copolymerization using HEMA and GMA with azobisisobutyronitrile (AIBN) as the initiator in ethanol; the titania sol was prepared by using the sol–gel method. The two kinds of solutions were spin-coated at 3000 rpm for 60 s. Different thicknesses of films were achieved by changing the concentration of the solutions and the spin-coating rate. The polymer layer was heated at 135 °C for 10 min to eliminate the solvent. The inorganic titania layer was heated at 60 °C for 10 min in order to solidify the layer and eliminate small organic molecules and solvent. The first layer was polymer and the last layer was titania in all our experiments and the total number of layers was 2*N*. Supporting Information Figure S1 gives the IR spectra of the titania sol film and polymer film. From these we can see that the titania sol and the polymer were successfully prepared, and the monomer left in the polymer film was eliminated successfully.

Figure 1a shows the transmission electron microscopy (TEM) image of the titania sol film, from which we can see that the titania sol has been transformed into titania nanoparticles. Figure 1b shows the cross-sectional scanning electron microscopy (SEM) image of a 1DPC of ten layers, from which we can see the multilayered structure of the 1DPC. The

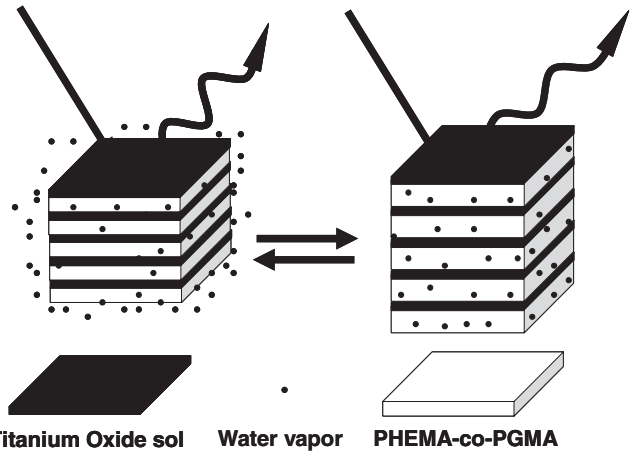

Scheme 1. Schematic image of organic/inorganic hybrid 1DPCs by alternated spin-coating of titania sol and PHEMA-co-PGMA.

© 2010 WILEY-VCH Verlag GmbH & Co. KGaA, Weinheim

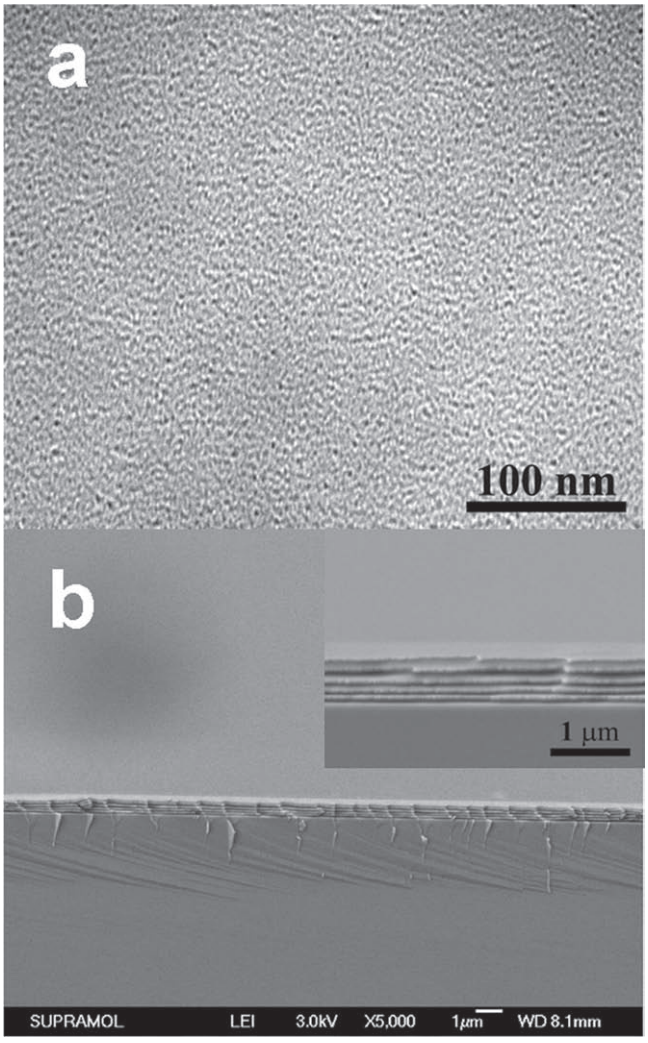

Figure 1. a) TEM image of titania layer. b) Cross-sectional SEM images of a 1DPC with ten layers; the inset is a magnified image.

enlarged image illustrates that the thickness of the same material is uniform and the whole material is made up of uniform multilayered structure over a large area. The inset of Figure 1b shows that both of the two materials contain five layers, and the average thicknesses of the polymer layer and titania layer are 99 and 46 nm, respectively, which agree with the thicknesses we measured using a surface profiler (109 and 49 nm, respectively). Some polymer layers are vacant, which may be caused by polymer shrinkage during vacuumizing.

2.2. Evolution of Optical Properties of the 1DPCs

The position of the Bragg peak and the stop-band width of 1DPCs can be calculated by using the following formulas:[34,35]

$$m\lambda_{\text{Bragg}} = 2D\sqrt{n_{\text{eff}}^2 - \sin^2\theta} \quad (1)$$

$$n_{\text{eff}}^2 = n_1^2 f_1 + n_2^2 f_2 \quad (2)$$

$$W = \frac{4}{\pi}\lambda_{\text{Bragg}}\left|\frac{n_2 - n_1}{n_2 + n_1}\right| \quad (3)$$

where m is the diffraction order, D is the period, λ_{Bragg} is the position of Bragg peak, θ is the incident angle, n_{eff} is the effective refractive index, W is the stop bandwidth, and n_1, f_1, n_2 and f_2 are the refractive indexes and volume fractions of the two different layers. From the equations above, we can conclude that the optical properties of 1DPCs can be tuned by changing the number of layers, incident angles, period, and refractive index. Meanwhile, we can also calculate the position of Bragg peak and the width of the stop band of the 1DPCs using the equations.

2.2.1 Number of Layers

Tuning optical properties of the 1DPCs can be achieved by increasing the number of layers (2N), which is shown in **Figure 2**. An intense (above 96% reflectance for 1DPCs made of 16 layers or more) and wide Bragg peak (at 504 nm) is observed, which is a direct consequence of the large contrast in refractive index between the titania layer and the polymer layer. The photonic bandwidth becomes narrower and the intensity of the peak grows with increasing numbers of layers, which is in good agreement with the previous theory describing the thickness dependence of the optical response of photonic crystal slabs.[36]

2.2.2 Incident Angle

A change of incident angles also influences the optical properties of 1DPCs. When increasing incident angles, the reflected wavelengths shift towards the shorter (blue/UV) end of the spectrum, which is a typical feature of 1DPCs. **Figure 3a** shows the effect of varying incident angles on the optical properties of 1DPCs. When incident angles are 30°, 45°, and 60°, the positions of the Bragg peaks are 616, 578, and 546 nm, respectively. Photographs of the 1DPCs at different angles are shown in Figure 3b. When incident angles are 30°, 45°, and 60°, the colors of the 1DPCs are red, yellow-green, and dark green, respectively. From Equation (1), we can see that the position of the Bragg peak decreases with increasing incident angles, which is in accordance with the experimental results shown in Figure 3a.

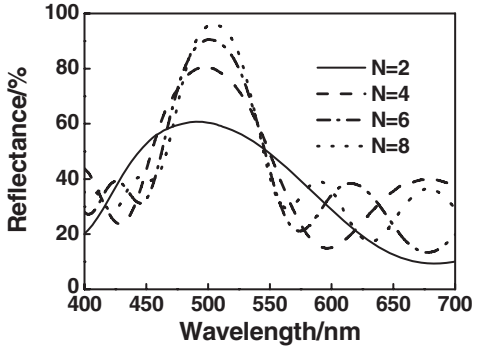

Figure 2. Optical properties of the 1DPCs with total numbers of layers (2N).

© 2010 WILEY-VCH Verlag GmbH & Co. KGaA, Weinheim

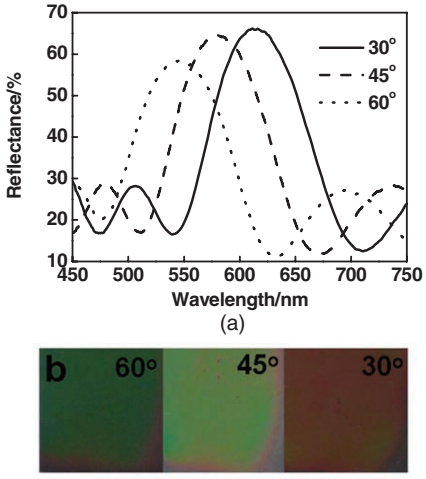

Figure 3. a) Optical properties of the 1DPCs with incident angles; b) color variation of the 1DPCs with incident angles; the scale bar represents 10 mm. The total number of layers (2*N*) is ten.

2.2.3 Layer Thickness

Equation (1) also reveals that the optical properties of 1DPCs can be tuned by changing the period. By increasing the period, the position of Bragg peak will shift to the red. By choosing proper periods, the position of the Bragg peak can be tuned through the whole visible spectral range. In accordance with the Bragg equation for 1DPCs in Equation (1), the spectral position of the fundamental Bragg peaks can be tuned by manipulating the geometric or optical thicknesses of the layers constituting the 1D photonic lattice. The thicknesses of the layers can be readily controlled by manipulating either the concentration of the polymer precursor solution and titania sol or the spin-coating rate of the deposition. As shown in the reflectance spectra (**Figure 4a**), fixing the thickness of titania layer at 49 nm while changing the thickness of the polymer layer from 91 to 110, 123, and 142 nm gives Bragg peak positions at 461, 520, 571, and 626 nm, respectively. The corresponding positions of Bragg peaks calculated from Equation (1) are 457, 514, 553, and 611 nm, respectively, which agree with the experimental results. Figure 4b shows that when fixing the polymer layer thickness at 123 nm and changing the titania layer thickness to 28, 39, 49, and 60 nm gives Bragg peak positions at 491, 535, 583, and 631 nm, respectively. The calculated positions of these Bragg peaks are 476, 513, 554, and 594 nm, respectively, which are consistent with the experimental results. Increasing the thickness of either the polymer or the titania layer broadens the bandwidth. This alteration is because the bandwidth is proportional to the position of the Bragg peaks, from Equation (3), while the position of the Bragg peak is proportional to the period, from Equation (1). Figure 4c illustrates the relationship between the thickness of the layers and the position of the Bragg peak. We can see that the Bragg peak positions increase in wavelength

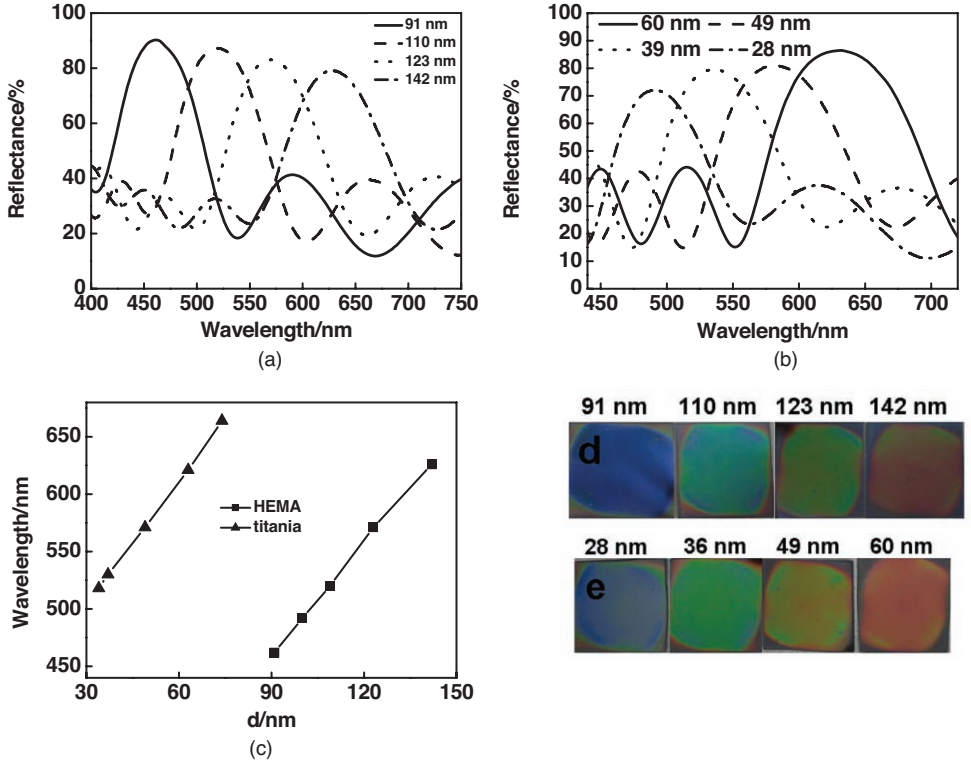

Figure 4. a) Optical properties of the 1DPCs with thickness of polymer layer; b) optical properties of the 1DPCs with thickness of titania layer; c) relationship between positions of the stop band with thickness of the layers; d) photographs of 1DPCs when the titania layer is 49 nm and the polymer layers are 91, 110, 123, and 142 nm; the scale bar represents 10 mm; e) photographs of 1DPCs when the polymer layer is 123 nm and titania layers are 28, 39, 49, and 60 nm; the scale bar represents 10 mm. The total number of layers (2*N*) is ten.

© 2010 WILEY-VCH Verlag GmbH & Co. KGaA, Weinheim

directly proportionally to the increase in thickness of one layer, while keeping the other layer constant. When the period is not changed very much, the n_{eff} changes little, from Equation (2). So from Equation (1), it can be easily seen that by increasing the thickness of one layer, the Bragg peak position shifts to the red in a linear way.

The 1DPCs prepared display uniform colors over a large area with minimal accidental striations and cracks as can be discerned from the photographs shown in Figure 4d and Figure 4e. The colors of the 1DPCs change from blue to red with the increase of the period and the reflectance spectra can span the whole visible spectra range. Fixing the thickness of the titania layer at 49 nm and changing the thickness of the polymer layer from 91 nm to 110, 123, and 142 nm, produces colors of the 1DPCs that are blue, green, yellow –green, and red, respectively, thereby covering the whole visible spectral range; fixing the polymer layer at 123 nm and changing the titania layer to 28, 39, 49, and 60 nm, gives 1DPCscolors of blue, green, orange, and red, respectively, again covering the whole visible spectral range. Other colors can also be obtained by tuning the thicknesses of the polymer or the titania layer. In our experiments, color uniformity can be achieved over an area of at least 20 mm × 20 mm. The 1DPCs can retain its color unvaried for at least half a year, which is explained by the perfect stability of the prepared materials and microstructures.

2.3. Responsiveness of 1DPCs to Water Vapor

From Eqution (1), it can be seen that the reflectance spectra and colors of 1DPCs can be tuned by changing the geometric thicknesses or optical thicknesses of the layers constituting the 1DPCs. Due to the hydrophility of PHEMA-co-PGMA, the 1DPCs are water-vapor responsive. Upon exposure of the 1DPCs to water vapor, swelling of the polymer layers results in an increase of the period of the 1DPCs, so the photonic stop band shifts to longer wavelength. The strong interaction between the hydroxy group of the polymer and the Ti–O group of the inorganic matrix through hydrogen bonding prevents swelling parallel to the substrate and confines the volume change in the swelling to one dimension; normal to the surface.[37] During swelling the titania layers maintain an unvaried thickness, while the polymer layers swell and change their refractive indexes.

When the water-vapor volume fraction is 0.0223, the position of the Bragg peak changes from 470 to 620 nm (**Figure 5a**). The color can come back to the original state immediately when the 1DPCs are exposed to air. From the reflectance spectra we can also see that the position of the Bragg peaks changes from 469 to 498 nm in 5 s and to 522 nm in 20 s, with the color changing from blue to blue –green, and then to green. This fast color-changing behavior and the shift of the stop band from blue to red in a short time are just like some photonic structural colors in nature, such as in the paradise whiptail.[11] A gradual increase of the bandwidth can be observed with an increase in the response time, which is mainly because of the increase in the refractive index difference between the titania layer and the polymer layer, as well as the increase in thickness of the polymer layer as more water vapor is incorporated into that layer. The response kinetics are shown in Figure 5b; it can be seen that the change of the stop band takes place very fast at first, and then reaches a balance and remains unvaried after the response time increases to 150 s.

The response sensitivity is another important parameter in the evaluation of sensing performance of the 1DPCs for some sensor applications. The sensitivity of the 1DPCs to water vapor is illustrated in **Figure 6a**. When the volume percentage of water vapor increases from 0.0108 to 0.0219, the position of the Bragg peak changes from 469 to 616 nm, which covers the entire visible spectra range. The bandwidth also gradually increases with increasing water-vapor concentration. The bandwidth broadening is mainly due to the increase of the difference in refractive index between the titania layer and the polymer layer and to the increasing thickness of the polymer layer as water vapor is incorporated into it. The color change of the 1DPCs with increasing water-vapor concentration is shown in Figure 6b. As the water-vapor volume fraction increases from 0.0108 to 0.0219, the color of the 1DPCs varies from blue to blue –green, dark green,

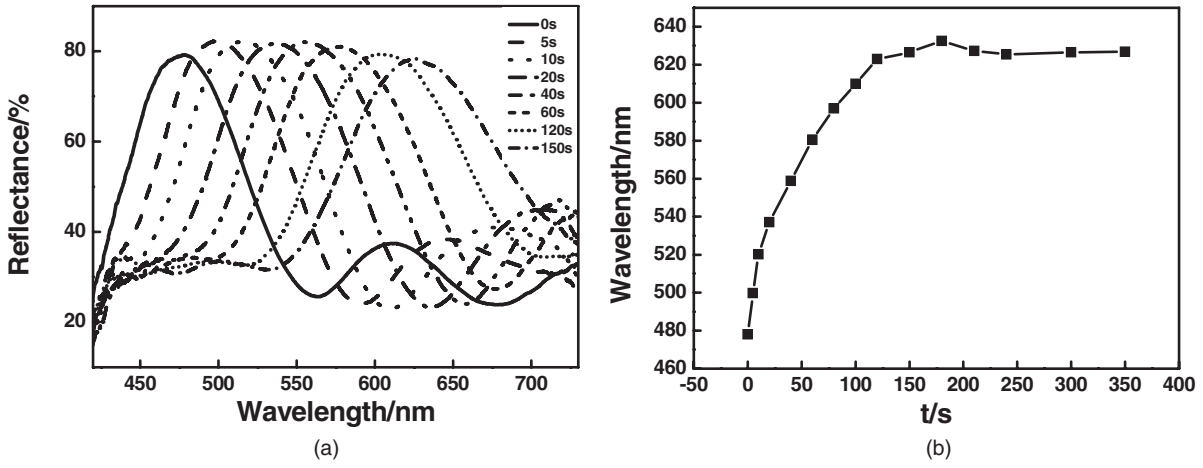

Figure 5. a) Optical properties of the 1DPCs with response time; b) relation between the position of the stop band with response time. The total number of layers (2*N*) is ten.

© 2010 WILEY-VCH Verlag GmbH & Co. KGaA, Weinheim

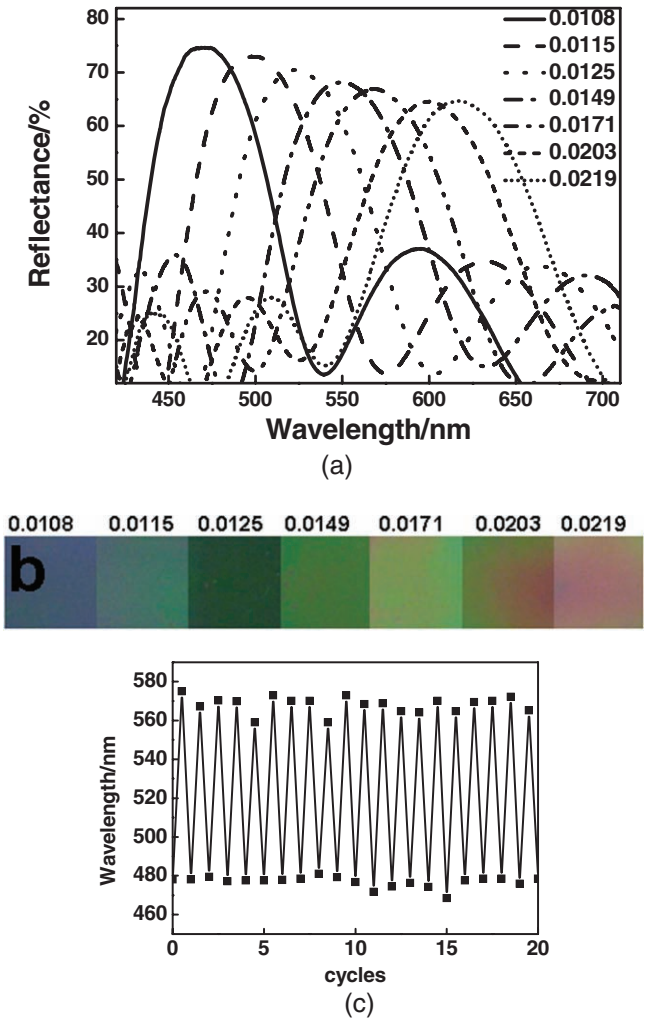

Figure 6. a) Sensitivity of the 1DPCs towards water vapor; b) color variation of the 1DPCs with water-vapor concentration, the scale bar represents 5 mm; c) swelling–deswelling cycles of the 1DPCs with water-vapor concentration at 0.0177. The total number of layers (2*N*) is ten.

green, yellow –green, and red, covering the whole visible range. The as-prepared 1DPCs successfully combine structural color and water-vapor sensitivity, which suggests these are promising materials for colorful detection of humidity. The repeatability of the 1DPCs' responsive behavior is very good. Figure 6c illustrates 20 cycles of the swelling–deswelling with little change in the stop band, and the water-vapor concentration being 0.0171. In our experiment we find this water-vapor-responsive behavior can be repeated over 100 times. The perfect repeating behavior illustrates the structure of 1DPCs is well maintained during the swelling–deswelling process.

3. Conclusion

In conclusion, bioinspired organic/inorganic hybrid 1DPCs are achieved by spin-coating titania and PHEMA-co-PGMA films alternately. The optical properties of 1DPCs can be tuned by changing the number of layers, period, and incident angles. By changing the period, the reflectance spectra of the 1DPCs can be made to span the whole visible range. The as-prepared 1DPCs exhibit reversible water-vapor sensitivity, evidenced by a distinct color change that covers the whole visible range. Considering sensitivity to water vapor, and the simple and low-cost fabrication approach, the 1DPCs are promising as an economical humidity sensor and display colorful detection possibilities in both chemical and biological fields in the future. Furthermore, by introducing other chemically or physically active materials into the one-dimensional photonic structure, lots of other responsive 1DPCs can be obtained, which opens up new approaches to displays, controllable release mechanisms, and optical devices.

4. Experimental Section

Materials: Glycidyl methacrylate (GMA, 99.5%) and 2-hydroxyethyl methacrylate (HEMA, 99.5%) were distilled under vacuum and stored at –15°C before use. AIBN was recrystalized twice in 95% ethanol before use. All other reagents were used as received. The silicon wafers (100) were cut into 20 mm × 20 mm pieces, soaked in a mixture of 98% H_2SO_4/30% H_2O_2 (volumetric ratio 7:3) for 20 min with boiling (caution: strong oxide), and then rinsed with deionized water several times, and lastly dried with an N_2 stream.

Synthesis of the Titania Sol: The titania sol was prepared according to reference [38]. Briefly, 4 mL tetrabutyl titanate was dissolved in 2 mL isopropanol (IPA) in a conical flask for 5 min. 0.21 g water and 17 µL concentrated HCl were mixed with 4 mL IPA for 5 min, then this solution was dripped into the above conical flask over about 10 min, and all were stirred for 12 h at room temperature. The copolymer was prepared by solution radical polymerization. In detail, 2 mL HEMA, 15 µL GMA, and 20 mg AIBN were dissolved into 20 mL ethanol, then the solution was bubbled with N_2 for 30 min and put into 60°C oil bath to react for 5 h. The solution was diluted using 20 mL alcohol and 5 mL water before use. In order to get different thicknesses of film, the titania sol was diluted with different volumes of IPA and the polymer solution was diluted with different volumes of ethanol before use.

Preparation of the 1DPCs: The 1DPCs were fabricated by spin-coating the titania sol and the polymer precursor alternately; both the titania sol and the polymer precursor were spin-coated at 3000 rpm for 60 s onto a silicon wafer. The titania layer was baked at 60°C for 10 min and the polymer layer was baked at 135°C for 10 min. The first layer was the polymer layer and the last layer was the titania layer in all our experiments. The number of total layers of the film materials was 2*N*.

Preparation of Water Vapor and Calculation of Its Concentration: Water vapor was introduced by bubbling nitrogen into water in a sealed glass. Its concentration was calculated by the formula: $M = P/P_0$(M, P, and P_0 represent the concentration of water vapor, partial pressure of water vapor and the total pressure, respectively).

Characterization: SEM micrographs were recorded with a JEOL FESEM 6700F electron microscope with a primary electron energy of 3 kV. The samples were sputtered with a thin layer of Pt prior to imaging. TEM micrographs were recorded with a RiLi H-800 electron microscope with accelerating voltage at 200 kV. A Shimadu 3600 UV-VIS-NIR spectrophotometer with standard mirror optics was used to measure the specular reflectance in the 200–1600 nm range at an incidence angle of 5°. An Optics spectrofluorometer (USB4000) was employed to detect the reflectance spectrum in the 400–750 nm at normal incidence. The angle-dependent specular reflection was evaluated using home-made equipment consisting of a collimated beam of a fiber-coupled tungsten–bromine lamp (Ocean Optics) and a goniometer (Rigaku), and the spectra were obtained using a spectrometer (Ocean Optics, USB650) from 400 to 800 nm. The ex-situ determination of layer thicknesses and optical constants of layers were carried out using an ellipsometer

© 2010 WILEY-VCH Verlag GmbH & Co. KGaA, Weinheim

(Woollam XLS-100) at an angle of 70° and within a spectral range of 315–720 nm. The thicknesses of the films were also determined using a Dektak150 surface profiler (Veeco).

Supporting Information

Supporting Information is available from the Wiley Online Library or from the author.

Acknowledgements

This work was supported by the National Science Foundation of China (Grant No. 20921003) and the National Basic Research Program of China (2007CB936402). The authors thank Dr. Qidai Chen, Yu Jin, and Qiang Gao for their technical support. This article is part of a Special Issue on Nanomaterials Research by Chinese Scientists.

Received: June 6, 2010
Published online: September 14, 2010

[1] E. Yablonovitch, *Phys. Rev. Lett.* **1987**, *58*, 2059.
[2] S. John, *Phys. Rev. Lett.* **1987**, *58*, 2486.
[3] J. D. Joannopoulos, P. R Villeneuve, S. Fan, *Nature* **1997**, *386*, 143.
[4] J. I. L. Chen, V. F. G. S. Y Choi, V. Kitaev, G. A. Ozin, *Adv. Mater.* **2006**, *18*, 1915.
[5] S. Nishimura, N. Abrams, B. A. Lewis, L. I. Halaoui, T. E. Mallouk, K. D. Benkstein, J. V. D. Lagemaat, A. J. Frank, *J. Am. Chem. Soc.* **2003**, *125*, 6306.
[6] A. C. Arsenault, D. P. Puzzo, I. Manners, G. A. Ozin, *Nat. Photonics.* **2007**, *1*, 468.
[7] a) J. M. Weissman, H. B. Sunkara, A. S. Tse, S. A. Asher, *Science.* **1996**, *274*, 959; b) J. H. Holtz, S. A. Asher, *Nature.* **1997**, *389*, 829.
[8] O. Sato, S. Kubo, Z. Z. Gu, *Acc. Chem. Res.* **2008**, *42*, 1.
[9] A. R. Parker, H. E. Townley, *Nat. Nanotechnol.* **2007**, *2*, 347.
[10] H. Kasukawa, N. Oshima, R. Fujii, *Zool. Sci.* **1987**, *4*, 243.
[11] L. M. Mathger, M. F. Land, U. E. Siebeck, N. J. Marshall, *J. Exp. Biol.* **2003**, *206*, 3607.
[12] a) Z. Z. Gu, A. Fujishima, O. Sato, *J. Am. Chem. Soc.* **2000**, *122*, 12387; b) S. Kubo, Z. Z. Gu, K. Takahashi, A. Fujishima, H. Segawa, O. Sato, *J. Am. Chem. Soc.* **2004**, *126*, 8314; c) E. T. Tian, J. X. Wang, Y. M. Zheng, Y. L. Song, L. Jiang, D. B. Zhu, *J. Mater. Chem.* **2008**, *18*, 1116.
[13] a) C. E. Reese, A. V. Mikhonin, M. Kamenjicki, A. Tikhonov, S. A. Asher, *J. Am. Chem. Soc.* **2004**, *126*, 1493; b) Z. Y. Ren, X. M. Zhang, J. H. Zhang, X. Li, X. Q. Pan, X. Fei, Z. C. Cui, B. Yang, *J. Mater. Chem.* **2008**, *18*, 3536.
[14] a) M. Ibisate, D. Glomayo, C. López, *Adv. Mater.* **2009**, *21*, 2899; b) N. Tetreault, H. Miguez, G. A. Ozin, *Adv. Mater.* **2004**, *16*, 1471.
[15] a) A. R. Parker, *Nature*, **2001**, *409*, 36; b) D. W. Lee, *Nature*, **1991**, *349*, 260; c) M. F. Land, *J. Exp. Biol.* **1966**, *45*, 433.
[16] L. D. Bonifacio, B. V. Lotsch, D. P. Puzzo, F. Scotognella, G. A. Ozin, *Adv. Mater.* **2009**, *21*, 1641.
[17] a) S. Y. Choi, M. Mamak, G. von Freymann, N. Chopra, G. A. Ozin, *Nano Lett.* **2006**, *6*, 2456; b) M. C. Fuertes, F. J. López–Alcaraz, M. C. Marchi, H. E. Troiani, V. Luca, H. Míguez, G. J. de, A. A. Soler-Illia, *Adv. Funct. Mater.* **2007**, *17*, 1247.
[18] a) S. Colodrero, M. Ocana, H. Míguez, *Langmuir.* **2008**, *24*, 4430; b) Z. Wu, D. Lee, M. Rubner, R. E. Cohen, *Small* **2007**, *3*, 1445.
[19] B. V. Lotsch, G. A. Ozin, *Adv. Mater.* **2008**, *20*, 4079.
[20] A. Janshoff, K. P. S. Dancil, C. Steinem, D. P. Greiner, V. S.-Y. Lin, C. Gurtner, K. Motesharei, M. J. Sailor, M. R. Ghadiri, *J. Am. Chem. Soc.* **1998**, *120*, 12108.
[21] D. L. Guo, L. X Fan, F. H. Wang, S. Y. Huang, X. W. Zou, *J. Phys. Chem. C.* **2008**, *112*, 17952.
[22] a) M. Karaman, S. E. Kooi, K. K. Gleason, *Chem. Mater.* **2008**, *20*, 2262. b) A. Convertino, A. Capobianchi, A. Valentini, E. N. M. Cirillo, *Adv. Mater.* **2003**, *15*, 1103; c) C. Kang, E. Kim, H. Baek, K. Hwang, D. Kwak, Y. Kang, and E. L. Thomas, *J. Am. Chem. Soc.* **2009**, *131*, 7538.
[23] a) D. J. Broer, J. Lub, G. N. Mol, *Nature.* **1995**, *378*, 467; b) B. Park, M. Kim, S. W. Kim, W. Jang, H. Takezoe, Y. Kim, E. H. Choi, Y. H. Seo, G. S. Cho, S. O. Kang, *Adv. Mater.* **2009**, *21*, 771.
[24] a) Y. Kang, J. J. Walish, T. Gorishnyy, E. L. Thomas, *Nat. Mater.* **2007**, *6*, 957; b) S. Valkama, H. Kosonen, J. Ruokolainen, T. Haatainen, M. Torkkeli, R. Serimaa, G. ten Brinke, O. Ikkala, *Nat. Mater.* **2004**, *3*, 872.
[25] L. Zhai, A. J. Nolte, R. E. Cohen, M. F. Rubner, *Macromolecules* **2004**, *37*, 6113.
[26] T. Kazmierczak, H. Song, A. Hiltner, E. Baer, *Macromol. Rapid. Commun.* **2007**, *28*, 2210.
[27] R. Jakubiak, T. J. Bunning, R. A. Vaia, L. V. Natarajan, V. P. Tondiglia, *Adv. Mater.* **2003**, *15*, 241.
[28] B. V. Lotsch, C. B. Knobbe, G. A. Ozin, *Small* **2009**, *5*, 1498.
[29] J. J. Walish, Y. Kang, R. A. Mickiewicz, E. L. Thomas, *Adv. Mater.* **2009**, *21*, 3078
[30] M. C. Fuertes, S. Colodrero, G. Lozano, A. R. González-Elipe, D. Grosso, C. Boissiére, C. Sánchez, G. J. de, A. A. Soler-Illia, H. Míguez, *J. Phys. Chem. C.* **2008**, *112*, 3157.
[31] S. Colodrero, M. Ocaña, A. R. González-Elipe, H. Míguez, *Langmuir* **2008**, *24*, 9135.
[32] a) R. Tominaga, M. Sivakumar, M. Tanaka, T. Kinoshita, *J. Mater. Chem.* **2008**, *18*, 976; b) V. K. S. Hsiao, K. T. Yong, A. N. Cartwright, M. T. Swihart, P. N. Prasad, P. F. Lloyd, T. J. Bunning, *J. Mater. Chem* **2009**, *19*, 3998.
[33] F. Scotognella, D. P. Puzzo, A. Monguzzi, D. S. Wiersma, D. Maschke, R. Tubino, G. A. Ozin, *Small* **2009**, *5*, 2048.
[34] V. Morandi, F. Marabelli, V. Amendola, M. Meneghetti, D. Comoretto, *Adv. Funct. Mater.* **2007**, *17*, 2779.
[35] B. Li, J. Zhou, L. Q. Li, Q. Li, S. Han, Z. B. Hao, *Chinese. Science. Bulletin.* **2005**, *50*, 1529.
[36] J. F. Bertone, P. Jiang, K. S. Hwang, D. M. Mittleman, V. L. Colvin, *Phys. Rev. Lett.* **1999**, *83*, 300.
[37] Q. Hu, E. Marand, *Polymer* **1999**, *40*, 4833.
[38] C. L. Lü, B. Yang, *J. Mater. Chem.* **2009**, *19*, 2884.

© 2010 WILEY-VCH Verlag GmbH & Co. KGaA, Weinheim